

Dynamics of a massive superfluid vortex in r^k confining potentials

Andrea Richaud,¹ Pietro Massignan,^{2,*} Vittorio Penna,³ and Alexander L. Fetter^{4,†}

¹*Scuola Internazionale Superiore di Studi Avanzati (SISSA), Via Bonomea 265, I-34136, Trieste, Italy*

²*Departament de Física, Universitat Politècnica de Catalunya, Campus Nord B4-B5, E-08034 Barcelona, Spain*

³*Dipartimento di Scienza Applicata e Tecnologia, Politecnico di Torino,*

Corso Duca degli Abruzzi 24, I-10129 Torino, Italy

⁴*Departments of Physics and Applied Physics, Stanford University, Stanford, CA 94305-4045, USA*

(Dated: August 8, 2022)

We study a superfluid vortex in condensate a trapped in a two-dimensional power-law potential $\propto r^k$. The vortex acquires a mass due to the presence of a condensate b of distinguishable atoms located in its core. The axisymmetry allows us to reduce the coupled dynamical equations of motion to a single radial equation with an effective potential V_{eff} . In many cases, V_{eff} has a single minimum, where the vortex precesses uniformly. A positive vortex with small mass orbits in the positive direction, but the sense of precession can reverse as the core mass increases.

I. INTRODUCTION

Superfluid vortices have been of great interest ever since Feynman's seminal article in 1955 [1]. The creation of ultracold atomic Bose-Einstein condensates (BECs) in 1995 [2, 3] greatly broadened the original focus on liquid ^4He . The first BEC vortex was in a two-component condensate with two trapped hyperfine states of ^{87}Rb [4, 5], although most subsequent experiments studied simpler one-component BECs.

In these mixtures, each component had its own resonant frequency and could be imaged separately, allowing nondestructive visualization of the large filled core, whose radius was larger than the wavelength of the imaging light (usually in the visible range). Consequently, it was feasible to study the precession of two-component vortices in real time [5]. In contrast, the empty core of a one-component vortex typically has a radius smaller than the wavelength of light and is observable only after free expansion by turning off the trap. Various methods subsequently allowed direct real-time observation of precession of a one-component vortex, the most direct visualizing the dynamics through expansion of successive small fractions of the condensate [6, 7]. Collisions between vortices have also been studied in great detail [8]. Soon after the first experiments, theoretical studies used a time-dependent variational Lagrangian to study the precession of one-component and two-component vortices [9, 10], although little detailed comparison was made with the experiments.

The dynamics of massive vortices has been object of various theoretical works over the last few years [11–14]. In these systems, the vortex in component a surrounds a localized massive core in component b , assuming interaction constants that favor phase separation of the two components. Our previous works focused on motion in a two-dimensional flat trap with a circular boundary

[11, 12]. Here we study a single vortex in a Thomas-Fermi condensate a , trapped in a power-law r^k potential. This model allows us to interpolate between the usual harmonic trap with $k = 2$ and the flat trap [15, 16] as the limit $k \rightarrow \infty$.

The paper is structured as follows: Section II relies on the Thomas-Fermi model in a power-law trap to find the condensate density for a single-component BEC. This result allows us to obtain a time-dependent variational Lagrangian, based on a trial function describing a single quantized vortex in a power-law potential, along with its opposite-sign image outside the condensate. The Lagrangian characterizes the dynamics of a single vortex, which here yields uniform circular precession. Section III adds the massive localized core to obtain the Lagrangian for a massive point vortex. In addition to the usual kinetic energy of the core mass, it also has a term linear in the vortex velocity. We discuss the analogy with the electromagnetic Lagrangian for a charged particle and find the associated effective magnetic field. The dynamics of a single massive point vortex typically involves uniform circular precession along with small stable oscillations around the local minimum in the effective potential. In some cases, however, this minimum disappears, and the vortex moves to the outer boundary. Positive massless vortices precess in the positive direction around the trap center, but we find that as their mass increases the precession frequency reverses sign. Such a striking feature may be detectable in current ultracold-atom experiments. We end with conclusions and outlook in Sec. IV.

II. THOMAS-FERMI MODEL FOR SINGLE-COMPONENT BEC

We rely on the familiar Gross-Pitaevskii (GP) model for the a -component condensate, assumed to be in the Thomas-Fermi (TF) limit. We also assume a quasi-two-dimensional system on the xy plane with central thickness d_z . For any axisymmetric potential $V_{\text{tr}}(r)$, the TF

* pietro.massignan@upc.edu

† fetter@stanford.edu

condensate density $n_a(r)$ satisfies

$$\mu_a = V_{\text{tr}}(r) + gn_a(r), \quad (1)$$

where $g = g_a/d_z$ is the two-dimensional coupling constant and g_a is the usual three-dimensional a -component interaction constant. Here $\mu_a = gn_0$ is the chemical potential of the a component, and $n_0 = n_a(0)$ is the density at the center of the trap. If $n_a(r)$ vanishes at the TF radius R , then Eq. (1) implies that $gn_0 = V_{\text{tr}}(R)$. For a power-law potential $\propto r^k$ with $k > 1$, the trap potential can be rewritten as

$$V_{\text{tr}}(r) = gn_0(r/R)^k. \quad (2)$$

By construction, the TF density $n_a(r) = n_0[1 - (r/R)^k]$ vanishes at the TF radius. The total number of particles is $N_a = \int d^2r n_a(r)$, with the resulting k -dependent central density

$$n_0 = \frac{k+2}{k} \frac{N_a}{\pi R^2}, \quad (3)$$

where the numerical factor $(k+2)/k$ varies smoothly in going from a harmonic trap ($k=2$) to a flat trap ($k \rightarrow \infty$).

A. Time-dependent variational Lagrangian

To study the dynamics of a vortex in a power-law trap, we rely on the time-dependent variational Lagrangian, which has proven valuable in many aspects of BEC physics [17], instead of the more complete (but more complicated) GP equation. In this approach, one takes a trial wave function $\Psi_a(\mathbf{r}, \boldsymbol{\rho})$ for the a component that depends on the vortex position $\boldsymbol{\rho}$ as a time-dependent parameter, where we use $\mathbf{r} = (r, \theta)$ as a general coordinate and $\boldsymbol{\rho} = (\rho, \phi)$ for the position of the vortex. Use the trial function Ψ_a to evaluate the Lagrangian $L_a = T_a - E_a$ for the a component, where

$$T_a[\Psi_a] = \frac{i\hbar}{2} \int d^2r \left(\Psi_a^* \frac{\partial \Psi_a}{\partial t} - \frac{\partial \Psi_a^*}{\partial t} \Psi_a \right) \quad (4)$$

and

$$E_a[\Psi_a] = \int d^2r \left(\frac{\hbar^2}{2m_a} |\nabla \Psi_a|^2 + V_{\text{tr}} |\Psi_a|^2 + \frac{g}{2} |\Psi_a|^4 \right) \quad (5)$$

depend on the coordinate of the vortex $\boldsymbol{\rho}$ through Ψ_a .

We use the TF model, with $\sqrt{n_a(r)}$ as the amplitude of the trial function Ψ_a . We assume a single vortex at $\boldsymbol{\rho}$ with dimensionless charge $q = \pm 1$ and an opposite-charge image vortex at $\boldsymbol{\rho}' = \hat{\boldsymbol{\rho}} R^2/\rho$ outside the condensate. This image is necessary for a flat trap and it facilitates the comparison for general values of k . Let $S(\mathbf{r}, \boldsymbol{\rho})$ be the angle between the vector $\mathbf{r} - \boldsymbol{\rho}$ and the $\hat{\mathbf{x}}$ axis. We choose the trial function

$$\Psi_a(\mathbf{r}) = \sqrt{n_a(r)} e^{iq[S(\mathbf{r}, \boldsymbol{\rho}) - S(\mathbf{r}, \boldsymbol{\rho}')] } \quad (6)$$

which includes the phase of the vortex and its image. Unless otherwise specified, we will assume that $q = +1$ in the following.

The evaluation of T_a and E_a follows as in Ref. [18]. With our trial function (6), we find

$$T_a = \hbar q \dot{\boldsymbol{\rho}} \times \hat{\mathbf{z}} \cdot \int d^2r n_a(r) \frac{\mathbf{r} - \boldsymbol{\rho}}{|\mathbf{r} - \boldsymbol{\rho}|^2} \quad (7)$$

plus a similar term for the image vortex at $\boldsymbol{\rho}'$. The integral in (7) is a vector that must lie along $\dot{\boldsymbol{\rho}}$ by symmetry, so that

$$T_a = \hbar q \dot{\boldsymbol{\rho}} \times \hat{\mathbf{z}} \cdot \hat{\boldsymbol{\rho}} \int d^2r n_a(r) \frac{r \cos \theta' - \rho}{r^2 - 2r\rho \cos \theta' + \rho^2},$$

where $\theta' = \theta - \phi$. The angular integral gives $-(2\pi/\rho)\Theta(\rho - r)$ where Θ is a unit step function that vanishes for $r > \rho$. A straightforward calculation gives

$$T_a(\rho, \dot{\phi}) = -q\hbar\pi n_0 R^2 \dot{\phi} \tau(\tilde{\rho}) \quad (8)$$

where $\tilde{\rho} = \rho/R$ is the dimensionless scaled radial vortex position and

$$\tau(\rho) = 2 \int_0^\rho r dr (1 - r^k) = \rho^2 - \frac{2\rho^{k+2}}{k+2} \quad (9)$$

is a dimensionless function of ρ . We now drop the tilde and treat ρ as dimensionless. By construction, note that $0 \leq \tau(\rho) < 1$ and

$$\frac{\tau'(\rho)}{\rho} = \frac{2n_a(\rho)}{n_0} = 2(1 - \rho^k). \quad (10)$$

A similar analysis for the contribution of the image vortex gives $\dot{\phi}$ multiplied by a constant because the image vortex lies outside the condensate. Since this contribution is a perfect time derivative, we can ignore it and retain only Eq. (8).

The remaining term is the energy of the vortex in Eq. (5). With our TF trial function, E_a is the kinetic-energy density of the vortex and its image integrated over the condensate density

$$E_a = \frac{\hbar^2}{2m_a} \int d^2r n_a(r) |\mathbf{v}(\mathbf{r}) - \mathbf{v}'(\mathbf{r})|^2, \quad (11)$$

where

$$\mathbf{v}(\mathbf{r}) = \hat{\mathbf{z}} \times \frac{\mathbf{r} - \boldsymbol{\rho}}{|\mathbf{r} - \boldsymbol{\rho}|^2} = \hat{\mathbf{z}} \times \nabla \ln |\mathbf{r} - \boldsymbol{\rho}| \quad (12)$$

is the dimensionless flow velocity of a vortex at $\boldsymbol{\rho}$ and \mathbf{v}' is the corresponding flow velocity of the image vortex at $\boldsymbol{\rho}'$. Here, the last form uses the alternative representation involving the stream function $\ln |\mathbf{r} - \boldsymbol{\rho}|$. A lengthy analysis gives

$$E_a(\rho) = \frac{\hbar^2 \pi n_0}{m_a} \epsilon(\rho), \quad (13)$$

where

$$\begin{aligned} \epsilon(\rho) = & \ln\left(\frac{1-\rho^2}{\delta(\rho)}\right) + \frac{\rho^k}{2} \ln\left(\frac{\delta(\rho)^2}{2\rho^2}\right) \\ & + \frac{\rho^k}{2} \left\{ H_{k/2} + H_{-k-2} + (-1)^k \left[\hat{B}_{-1} - \hat{B}_{-1/\rho} \right] \right. \\ & + B_\rho(-k-1, 0) + \frac{2\rho^2}{k+2} \left[2\hat{F}(\rho^2) - \rho^2\hat{F}(\rho^4) \right] \left. \right\} \\ & + \frac{1}{2\rho^k} \left\{ \hat{B}_{\rho^2} - \hat{B}_\rho + (-1)^k \left[\hat{B}_{-\rho} - \hat{B}_{-\rho^2} \right] \right\} \quad (14) \end{aligned}$$

with ρ again dimensionless. Here H_n denotes the harmonic number, $B_\rho(k, \alpha)$ is the incomplete beta function [and we often used the shorthand notation $\hat{B}_\rho \equiv B_\rho(k+2, 0)$],

$$\hat{F}(\rho) = {}_2F_1\left(1, \frac{k}{2} + 1, \frac{k}{2} + \frac{1}{2}; \rho\right)$$

is a hypergeometric function, and $\delta(\rho) = \delta_0 \sqrt{n_0/n_a(\rho)}$ with δ_0 a constant of order $\xi_0/R \approx 0.01$.

B. Dynamical motion of a vortex

It is now convenient to introduce dimensionless variables, with R as the length scale, $m_a R^2/\hbar$ as the time scale and $\hbar^2 \pi n_0/m_a$ as the energy scale. In this way we have the very simple dimensionless Lagrangian for the pure a -component vortex

$$L_a(\rho, \dot{\phi}) = -q\tau(\rho)\dot{\phi} - \epsilon(\rho). \quad (15)$$

This Lagrangian conserves the angular momentum $l = \partial L_a/\partial \dot{\phi} = -q\tau(\rho)$, so that the vortex precesses at fixed ρ . Note that by construction a massless positive vortex has always $l < 0$. The precession rate $\dot{\phi}$ follows from $\partial L_a/\partial \rho = -q\tau'(\rho)\dot{\phi} - \epsilon'(\rho) = 0$ with the dimensionless angular speed

$$\Omega = \dot{\phi} = -\frac{\epsilon'(\rho)}{2q\rho(1-\rho^k)}. \quad (16)$$

Since ϵ' is negative while $\rho(1-\rho^k)$ is positive, a massless vortex precesses in the same sense as its circulation q .

For a flat potential ($k \rightarrow \infty$), we have $\epsilon_\infty = \ln(1-\rho^2)$, reproducing the usual result

$$\Omega_\infty = \frac{\hbar}{m_a R^2} \frac{1}{1-\rho^2}, \quad (17)$$

now rewritten in conventional units. For the harmonic potential with $k=2$, we have

$$\epsilon_2 = (1-\rho^2) \left[\frac{(1+\rho^2)\ln(1-\rho^2)}{2\rho^2} - \ln\delta(\rho) \right], \quad (18)$$

where the vortex-core cutoff $\delta(\rho)$ depends on the condensate density and is scaled with R .

Figure 1 shows the precession rate of a vortex in a single-component BEC for selected integer values of k as a function of the vortex position ρ . The solid curves show Eq. (16) for the massive point vortex model studied here. The dots show the results from the time-dependent Gross-Pitaevskii equation (solved using variants of algorithms we employed in Ref. [12]). The close overlap between lines and dots confirms the accuracy of the time-dependent variational Lagrangian formalism.

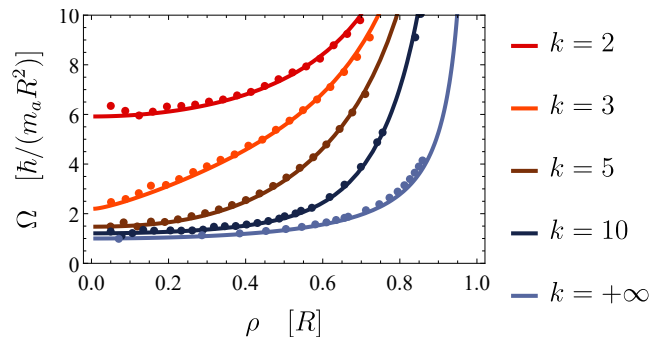


FIG. 1. Dimensionless precession frequency Ω for a vortex located at distance ρ from the center of a single-component BEC in a power-law r^k trap. Solid lines are the analytic predictions of Eq. (16), while dots show results from the full time-dependent GP equation. The value of k increases going from the top curve to the bottom curve.

For comparison with the study of the dynamics of a massive point vortex, which will be discussed in Sec. III, it is valuable to rewrite Eq. (15) in vector form

$$L_a = q \frac{\tau(\rho)}{\rho} \dot{\boldsymbol{\rho}} \times \hat{\boldsymbol{\rho}} \cdot \hat{\boldsymbol{z}} - \epsilon(\rho). \quad (19)$$

The corresponding canonical momentum

$$\mathbf{p}_a = \frac{\partial L_a}{\partial \dot{\boldsymbol{\rho}}} = q \frac{\tau(\rho)}{\rho} \hat{\boldsymbol{\rho}} \times \hat{\boldsymbol{z}} = -q \frac{\tau(\rho)}{\rho} \hat{\boldsymbol{\phi}} \quad (20)$$

is in the azimuthal direction, as expected for uniform circular motion. Note that the angular momentum is $\mathbf{l} = \boldsymbol{\rho} \times \mathbf{p}_a = -q\tau(\rho)\hat{\boldsymbol{z}}$, as found earlier.

The dynamics for this massless vortex follows from $\dot{\mathbf{p}}_a = \partial L_a/\partial \boldsymbol{\rho}$, which gives

$$\dot{\mathbf{p}}_a = q \left(\frac{\tau(\rho)}{\rho^2} - \frac{\tau'(\rho)}{\rho} \right) (\dot{\boldsymbol{\rho}} \cdot \hat{\boldsymbol{\phi}}) \hat{\boldsymbol{\rho}} - \epsilon'(\rho)\hat{\boldsymbol{\rho}}. \quad (21)$$

For uniform circular motion at fixed ρ , we have $\dot{\mathbf{p}}_a = q[\tau(\rho)/\rho]\dot{\boldsymbol{\phi}}\hat{\boldsymbol{\rho}}$, so that some terms cancel. As a result, we find

$$0 = [2q(1-\rho^k)(\dot{\boldsymbol{\rho}} \times \hat{\boldsymbol{z}} \cdot \hat{\boldsymbol{\rho}}) - \epsilon'(\rho)] \hat{\boldsymbol{\rho}}. \quad (22)$$

The last term is the “force” arising from the negative gradient of the energy $\epsilon(\rho)$. In this picture, the vortex moves to ensure that the total force vanishes, which is precisely the “Magnus” effect. The resulting precession frequency reproduces the result given in Eq. (16), which follows more directly from the Lagrangian dynamics.

III. MASSIVE POINT VORTEX MODEL

In our model for a massive point vortex, the total Lagrangian is the previous L_a for the a component augmented by the Lagrangian L_b for the b component. As discussed in detail in Ref. [12], L_b is proportional to N_b , with a kinetic term $\frac{1}{2}N_b m_b \dot{\boldsymbol{\rho}}^2$. The new feature here is the trap potential, so that $L_b = \frac{1}{2}N_b m_b \dot{\boldsymbol{\rho}}^2 - N_b V_{\text{tr}}(\rho)$. With our dimensionless variables, \bar{L}_b is

$$L_b = \frac{1}{2}\mathbf{m}\dot{\boldsymbol{\rho}}^2 - \nu\rho^k = \frac{1}{2}\mathbf{m}(\dot{\rho}^2 + \rho^2\dot{\phi}^2) - \nu\rho^k, \quad (23)$$

where $\mathbf{m} = M_b/M_a = N_b m_b/(N_a m_a)$ is the ratio of the total b mass to the total a mass, and $\nu = N_b g m_a/(\hbar^2 \pi)$. Note that ν is proportional to the product $N_b g$ and independent of n_0 .

A. Total Lagrangian for massive point vortex

In this way the Lagrangian L for a single massive point vortex becomes

$$L = \frac{1}{2}\mathbf{m}(\dot{\rho}^2 + \rho^2\dot{\phi}^2) - q\tau(\rho)\dot{\phi} - \epsilon(\rho) - \nu\rho^k, \quad (24)$$

here written in coordinate form. It is helpful also to rewrite L in vector form as

$$L = \frac{1}{2}\mathbf{m}\dot{\boldsymbol{\rho}}^2 - q\frac{\tau(\rho)}{\rho}\dot{\boldsymbol{\rho}} \cdot \hat{\boldsymbol{\phi}} - \epsilon(\rho) - \nu\rho^k. \quad (25)$$

It has an unusual structure in that it has a term linear in the generalized velocity in addition to the usual quadratic terms proportional to the inertial mass.

Such a Lagrangian is reminiscent of the Lagrangian L_{em} for a charged particle at $\boldsymbol{\rho}$ in an electromagnetic field

$$L_{\text{em}} = \frac{1}{2}\mathbf{m}\dot{\boldsymbol{\rho}}^2 + q\dot{\boldsymbol{\rho}} \cdot \mathbf{A} - q\Phi, \quad (26)$$

where q is the charge, \mathbf{A} is the vector potential and Φ is the scalar potential. The first terms of Eqs. (25) and (26) are the same. The second term of Eq. (25) arises from Eq. (19) which is linear in the vortex charge q . Comparison with (26) identifies the effective vector potential

$$\mathbf{A}_{\text{eff}}(\boldsymbol{\rho}) = -\frac{\tau(\rho)}{\rho}\hat{\boldsymbol{\phi}} = \pi\hbar n_0 R \frac{\tau(\rho)}{\rho}\hat{\boldsymbol{\rho}} \times \hat{\boldsymbol{z}}, \quad (27)$$

where the second form is in conventional units. It depends on both the local density and the exponent k . The third term of Eq. (25) arises from the energy (11) of the vortex and its image. It is quadratic in the vortex charge and hence proportional to q^2 , which here is simply 1. The last term in (25) is the trap potential and hence independent of q .

The effective magnetic field is

$$\mathbf{B}_{\text{eff}}(\boldsymbol{\rho}) = \nabla \times \mathbf{A}_{\text{eff}} = -2\pi\hbar n_a(\rho)\hat{\boldsymbol{z}}, \quad (28)$$

here expressed in conventional units. It is nonuniform except for a flat trap ($k \rightarrow \infty$), but the total flux obtained as $\int d^2\rho B_{\text{eff}}(\boldsymbol{\rho}) = -2\pi\hbar N_a$ is independent of k .

B. Dynamics of a massive point vortex

Since L is independent of ϕ , the angular momentum $l = \partial L/\partial\dot{\phi}$ of the massive vortex is conserved, with

$$l = \mathbf{m}\rho^2\dot{\phi} - q\tau(\rho). \quad (29)$$

Unlike the massless case, the angular momentum of a massive vortex can now have either sign. The associated radial motion follows directly as

$$\mathbf{m}\ddot{\rho} = \frac{\partial L}{\partial\rho} = \mathbf{m}\rho\dot{\phi}^2 - q\tau'(\rho)\dot{\phi} - \epsilon'(\rho) - k\nu\rho^{k-1}. \quad (30)$$

Some manipulation gives the equation of energy conservation

$$\frac{1}{2}\mathbf{m}\dot{\rho}^2 + V_{\text{eff}}(\rho) = \text{constant}, \quad (31)$$

with the effective potential

$$V_{\text{eff}}(\rho) = \frac{[l + q\tau(\rho)]^2}{2\mathbf{m}\rho^2} + \epsilon(\rho) + \nu\rho^k. \quad (32)$$

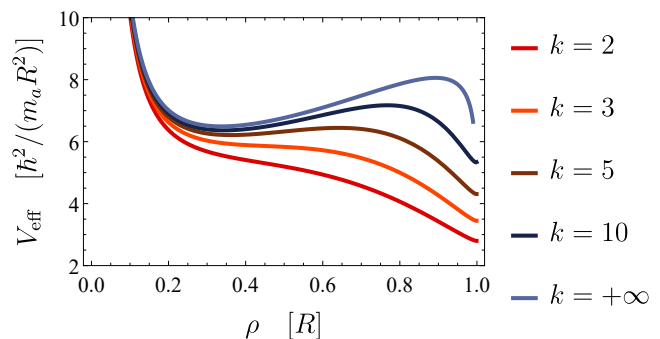


FIG. 2. Plot of the effective potential (32) as a function of the radial distance ρ , here shown for several values of k and fixed $l = \mathbf{m} = 0.1$ and $\nu = 1$. The value of k decreases going from the top curve to the bottom one.

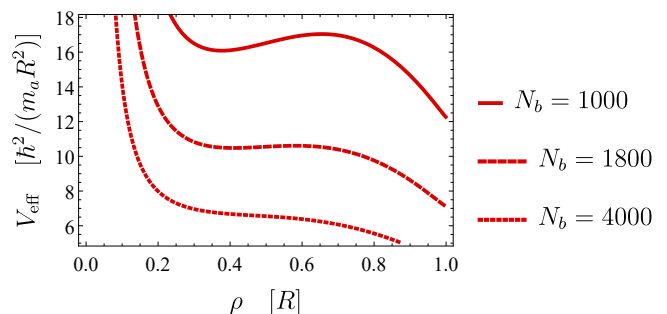


FIG. 3. Plot of the effective potential (32) as a function of the radial distance ρ , here expressed for several values of N_b and fixed $k = 2$, $l = 0.1$, $\mathbf{m} = 1.5 \times 10^{-5} N_b$, $\nu = 2.5 \times 10^{-4} N_b$.

In many cases, $V_{\text{eff}}(\rho)$ has a single local minimum at a position ρ_0 that depends on the parameters l , \mathbf{m} , and ν . Figure 2 shows that the presence of the minimum depends sensitively on k . For a given mass ratio \mathbf{m} the flat trap ($k \rightarrow \infty$) has a local minimum, but the latter disappears when k decreases beyond a critical value. The minimum also disappears as the number N_b of atoms in the core increases, as shown in Fig. 3.

For small $\mathbf{m} \ll 1$, we can ignore the last two terms of (32) and focus on the first term. If l is also small, the minimum occurs at small $\rho_0 \approx \sqrt{l}$, confirming that there is always a local minimum, as expected from the behavior for a pure a condensate.

If the effective potential has a local minimum at ρ_0 , a massive point vortex at this radial distance from the origin precesses uniformly at a rate obtained by setting the right side of Eq. (30) to zero. The resulting precession frequency Ω now satisfies a quadratic equation

$$\mathbf{m}\rho_0\Omega^2 - q\tau'(\rho_0)\Omega - \epsilon'(\rho_0) - k\nu\rho_0^{k-1} = 0. \quad (33)$$

The first and last terms arise from the presence of the vortex mass, since both \mathbf{m} and ν are proportional to N_b . In contrast, the second and third terms are just those studied in the previous section, including both the Magnus effect and the variational energy $\epsilon(\rho)$. Thus Eq. (33) includes all the physics inherent in our combined Lagrangian $L = L_a + L_b$.

For small N_b , both \mathbf{m} and ν are small, and the single root of Eq. (33) reproduces Eq. (16). As the core mass increases, Eq. (33) has two solutions, so that for a given ρ_0 there exist two distinct modes with different precession frequencies for a massive point vortex. With positive q , the larger root is

$$\Omega_+ = \frac{\tau'(\rho_0) + \sqrt{\tau'(\rho_0)^2 + 4\mathbf{m}\rho_0 [\epsilon'(\rho_0) + k\nu\rho_0^{k-1}]}}{2\mathbf{m}\rho_0}. \quad (34)$$

It diverges for small mass ratio $\mathbf{m} \ll 1$. For our purposes, the smaller root Ω_- is more physically significant because it remains finite for small \mathbf{m}

$$\Omega_- = \frac{2[-\epsilon'(\rho_0) - k\nu\rho_0^{k-1}]}{\tau'(\rho_0) + \sqrt{\tau'(\rho_0)^2 + 4\mathbf{m}\rho_0 [\epsilon'(\rho_0) + k\nu\rho_0^{k-1}]}}. \quad (35)$$

The denominator of Eq. (35) is generally positive (as discussed below, it can be complex, which implies instability). In contrast, the numerator can have either sign, depending on the vortex position ρ and the dimensionless parameter ν , which depends linearly on N_b . The quantity $-\epsilon'(\rho)$ is positive, but $-k\nu\rho^{k-1}$ is negative. For small ν , the energy term with ϵ' dominates and the positive massive vortex precesses in the positive sense. For larger ν , however, the derivative of the trap potential dominates, and a positive vortex now precesses in the negative direction. Figure 4 illustrates this situation for several integer values of k . Ruban [13] independently found similar behavior for $k = 2$ with a hydrodynamic

model based on two coupled GP equations. In our model of a massive point vortex, the effect is most pronounced for the harmonic trap ($k = 2$), and is absent for the flat trap ($k \rightarrow \infty$), as found in Ref. [12].

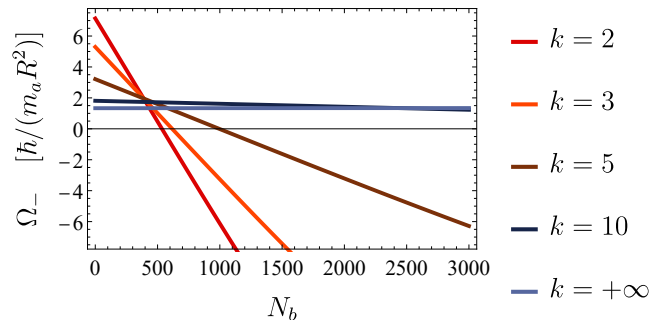


FIG. 4. The precession frequency Ω_- [see Eq. (35)] is positive for small core masses, but it can vanish and become negative as the number N_b of component- b core atoms increases. Here $\mathbf{m} = 3 \times 10^{-6} N_b$ and $\nu = 10^{-2} N_b$, which are typical values for a vortex in a BEC composed of 6×10^5 ^{23}Na atoms (pancake-shaped, with $R \sim 50 \mu\text{m}$ and $d_z \sim 1 \mu\text{m}$), with the vortex mass provided by N_b ^{39}K atoms. At $N_b = 0$ the value of k increases going from the top curve to the bottom curve.

To understand the connection between the two roots Ω_{\pm} and the single local minimum ρ_0 , we started from parameters \mathbf{m} , l and ν that give a clear minimum such as the upper curve in Fig. 3. These values then yield Ω_{\pm} from Eqs. (34) and (35). Use these frequencies to find the corresponding angular momenta l_{\pm} from (29). One of the solutions is the same as the input in finding the minimum of $V_{\text{eff}}(\rho)$, but the other solution gives a second distinct $V_{\text{eff}}(\rho)$. Although both effective potential curves have minima at the same ρ_0 , they have different l_{\pm} and therefore different detailed shapes.

As mentioned above, the two roots Ω_{\pm} are usually real, but they can become complex-conjugate pairs for some values of N_b , indicating that the vortex will not precess but instead drift to the outer boundary. In Ref. [12] we found this behavior for a flat trap, and we here generalize the discussion for general k .

Equation (33) has real coefficients, so that its roots are either real or complex conjugates, depending on the sign of the discriminant

$$\mathcal{D} = q^2\tau'(\rho_0)^2 + 4\mathbf{m}\rho_0 [\epsilon'(\rho_0) + k\nu\rho_0^{k-1}]. \quad (36)$$

The quantity $\epsilon'(\rho_0)$ is negative and $k\nu\rho_0^{k-1}$ is positive, so that their sum can have either sign. A numerical search for $k = 2$ readily finds regions of parameter space where \mathcal{D} is negative, similar to the situation for a flat trap [12].

C. Stability of uniform precession for massive vortex

If $V_{\text{eff}}(\rho)$ has a local minimum at ρ_0 , then the stability of the uniform precession follows by expanding around the minimum, with $\rho = \rho_0 + \delta$. Since $V'_{\text{eff}}(\rho_0)$ vanishes at a local minimum, the leading terms from Eq. (31) become

$$\mathbf{m}\ddot{\delta} + V''_{\text{eff}}(\rho_0)\delta. \quad (37)$$

This equation describes a simple harmonic oscillator with squared frequency

$$\omega^2 = \frac{V''_{\text{eff}}(\rho_0)}{\mathbf{m}}, \quad (38)$$

where the local curvature $V''_{\text{eff}}(\rho_0)$ serves as an effective spring constant. An equivalent procedure is to expand the pair of Euler-Lagrange equations for ρ and ϕ around the stable precessing motion; this latter approach shows that the perturbations in ρ and ϕ are out of phase by $\pi/2$. Figure 5 shows typical perturbed trajectories for both signs of the precession frequency Ω_- .

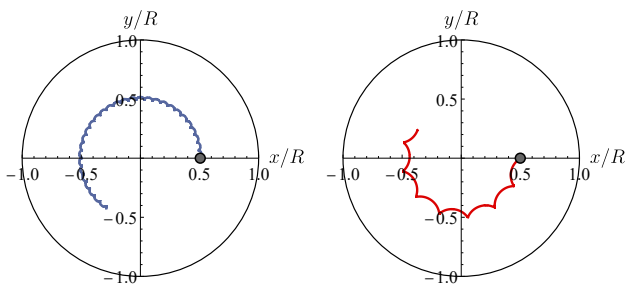


FIG. 5. Perturbed uniform circular orbits of a positive vortex for $k = \infty$ (left panel) and $k = 2$ (right panel). Black dots correspond to the initial positions. The precession frequency, given by Eq. (35), is positive in the first case and negative in the second. The frequency of small-amplitude radial oscillations is given by Eq. (38). Here we used $\mu = 0.03$, $\nu = 10$ and $\delta_0 = 0.005$.

Figures 2 and 3 indicate that the effective potential resembles a cubic curve with a single local minimum and a single local maximum. The local minimum (maximum) is stable (unstable) with positive (negative) curvature. As the parameters vary, the two stationary points can merge and form a single inflection point, which signals the onset of instability. Beyond this point, the radial position obeys the simple Newtonian dynamical equation $\mathbf{m}\ddot{\rho} = -V'_{\text{eff}}(\rho)$. In this case, the vortex will move to the outer boundary of the condensate.

IV. CONCLUSIONS AND OUTLOOK

In this paper, we constructed a two-dimensional Lagrangian $L = L_a + L_b$ for a massive point vortex in a

power-law trap potential $\propto r^k$. Our model assumes a singly quantized vortex in condensate a surrounding a localized condensate b that provides an inertial mass. The power-law potential allows an interpolation between the harmonic trap ($k = 2$) and the flat trap with a rigid circular boundary ($k \rightarrow \infty$). For an empty-core vortex in the pure a component, the model Lagrangian L_a leads to first-order dynamical equations with uniform circular precession for all values of k .

To include the inertial effect of the core, we added the Lagrangian L_b derived in [12], now generalized to the power-law trap. The total Lagrangian for the vortex coordinate $\boldsymbol{\rho} = (\rho, \phi)$ is axisymmetric and therefore conserves the total angular momentum l . Unusually, l includes not only the usual Newtonian inertial part $\propto \rho^2 \dot{\phi}$ but also a contribution from the vortex that is analogous to that for a charged particle in a nonuniform external magnetic field.

Manipulation of the coupled dynamical equations for ρ and ϕ leads to an effective potential $V_{\text{eff}}(\rho)$ and an explicit radial dynamical equation $\mathbf{m}\dot{\rho} = -V'_{\text{eff}}(\rho)$, where $\mathbf{m} = M_b/M_a$ is the mass ratio. For small enough values of \mathbf{m} and l , $V_{\text{eff}}(\rho)$ has a single local minimum, where stable uniform circular motion can occur. For larger \mathbf{m} , however, the local minimum disappears and the vortex spirals outward to the trap edge.

We studied the precession of a massive vortex for various values of the parameters in the Lagrangian such as the mass ratio $\mathbf{m} = M_b/M_a$, the coupling strength $\nu = N_b g m_a / (\hbar^2 \pi)$ between the vortex and the trap, and the exponent k of the trap potential. For a flat potential ($k \rightarrow \infty$), a positive massive vortex always precesses in the positive sense, independent of the number N_b of b -component atoms which provide its mass. For finite k , the precession can reverse direction with increasing N_b . The effect is stronger for smaller k , and therefore it should be most easily observable in the usual case of harmonic trapping ($k = 2$).

We note that early experiments [5] on a vortex in a two-component BEC with a large core found no such behavior. It would be very interesting to study similar systems with smaller core radii and ultimately detect the reversal of precession experimentally.

ACKNOWLEDGEMENTS

We thank Carlo Beenaker, Matteo Ferraretto, Giacomo Roati, Francesco Scazza, and Leticia Tarruell for stimulating discussions. P.M. was supported by grant PID2020-113565GB-C21 funded by MCIN/AEI/10.13039/501100011033, by the National Science Foundation under Grant No. NSF PHY-1748958, and by the *ICREA Academia* program.

-
- [1] R. P. Feynman, in *Progress in Low Temperature Physics*, Vol. 1 (Elsevier, North-Holland, Amsterdam, 1955) pp. 17–53.
- [2] C. J. Pethick and H. Smith, *Bose-Einstein Condensation in Dilute Gases* (Cambridge University Press, Cambridge, 2008) 2nd ed.
- [3] L. Pitaevskii and S. Stringari, *Bose-Einstein Condensation and Superfluidity* (Oxford University Press, Oxford, 2016) 2nd ed.
- [4] M. R. Matthews, B. P. Anderson, P. C. Haljan, D. S. Hall, C. E. Wieman, and E. A. Cornell, *Vortices in a Bose-Einstein Condensate*, *Phys. Rev. Lett.* **83**, 2498 (1999).
- [5] B. P. Anderson, P. C. Haljan, C. E. Wieman, and E. A. Cornell, *Vortex Precession in Bose-Einstein Condensates: Observations with Filled and Empty Cores*, *Phys. Rev. Lett.* **85**, 2857 (2000).
- [6] D. V. Freilich, D. M. Bianchi, A. M. Kaufman, T. K. Langin, and D. S. Hall, *Real-Time Dynamics of Single Vortex Lines and Vortex Dipoles in a Bose-Einstein Condensate*, *Science* **329**, 1182 (2010).
- [7] S. Serafini, L. Galantucci, E. Iseni, T. Bienaimé, R. N. Bisset, C. F. Barenghi, F. Dalfovo, G. Lamporesi, and G. Ferrari, *Vortex Reconnections and Rebounds in Trapped Atomic Bose-Einstein Condensates*, *Phys. Rev. X* **7**, 021031 (2017).
- [8] W. Kwon, G. Del Pace, K. Xhani, L. Galantucci, A. Muzi Falconi, M. Inguscio, F. Scazza, and G. Roati, *Sound emission and annihilations in a programmable quantum vortex collider*, *Nature* **600**, 64 (2021).
- [9] E. Lundh and P. Ao, *Hydrodynamic approach to vortex lifetimes in trapped Bose condensates*, *Phys. Rev. A* **61**, 063612 (2000).
- [10] S. A. McGee and M. J. Holland, *Rotational dynamics of vortices in confined Bose-Einstein condensates*, *Phys. Rev. A* **63**, 043608 (2001).
- [11] A. Richaud, V. Penna, R. Mayol, and M. Guilleumas, *Vortices with massive cores in a binary mixture of Bose-Einstein condensates*, *Phys. Rev. A* **101**, 013630 (2020).
- [12] A. Richaud, V. Penna, and A. L. Fetter, *Dynamics of massive point vortices in a binary mixture of Bose-Einstein condensates*, *Phys. Rev. A* **103**, 023311 (2021).
- [13] V. P. Ruban, *Direct and Reverse Precession of a Massive Vortex in a Binary Bose-Einstein Condensate*, *JETP Lett.* **115**, 415 (2022).
- [14] R. Doran, A. W. Baggaley, and N. G. Parker, *Vortex Solutions in a Binary Immiscible Bose-Einstein Condensate*, [arXiv:2207.12913](https://arxiv.org/abs/2207.12913) (2022).
- [15] N. Navon, R. P. Smith, and Z. Hadzibabic, *Quantum gases in optical boxes*, *Nat. Phys.* **17**, 1334 (2021).
- [16] Y.-Q. Zou, É. Le Cerf, B. Bakkali-Hassani, C. Maury, G. Chauveau, P. C. M. Castilho, R. Saint-Jalm, S. Nascimbene, J. Dalibard, and J. Beugnon, *Optical control of the density and spin spatial profiles of a planar Bose gas*, *J. Phys. B: At. Mol. Opt. Phys.* **54**, 08LT01 (2021).
- [17] V. M. Pérez-García, H. Michinel, J. I. Cirac, M. Lewenstein, and P. Zoller, *Low Energy Excitations of a Bose-Einstein Condensate: A Time-Dependent Variational Analysis*, *Phys. Rev. Lett.* **77**, 5320 (1996).
- [18] J.-K. Kim and A. L. Fetter, *Dynamics of a single ring of vortices in two-dimensional trapped Bose-Einstein condensates*, *Phys. Rev. A* **70**, 043624 (2004).